Surface Chemistry

International Edition: DOI: 10.1002/anie.201504761
German Edition: DOI: 10.1002/ange.201504761

Bioactive Seed Layer for Surface-Confined Self-Assembly of Peptides**

Cécile Vigier-Carrière, Tony Garnier, Déborah Wagner, Philippe Lavalle, Morgane Rabineau, Joseph Hemmerlé, Bernard Senger, Pierre Schaaf, Fouzia Boulmedais,* and Loïc Jierry*

Abstract: *The design and control of molecular systems that self-assemble spontaneously and exclusively at or near an interface represents a real scientific challenge. We present here a new concept, an active seed layer that allows to overcome this challenge. It is based on enzyme-assisted self-assembly. An enzyme, alkaline phosphatase, which transforms an original peptide, Fmoc-FFY(PO_4^{2-}), into an efficient gelation agent by dephosphorylation, is embedded in a polyelectrolyte multilayer and constitutes the "reaction motor". A seed layer composed of a polyelectrolyte covalently modified by anchoring hydrogelator peptides constitutes the top of the multilayer. This layer is the nucleation site for the Fmoc-FFY peptide self-assembly. When such a film is brought in contact with a Fmoc-FFY-(PO_4^{2-}) solution, a nanofiber network starts to form almost instantaneously which extents up to several micrometers into the solution after several hours. We demonstrate that the active seed layer allows convenient control over the self-assembly kinetics and the geometric features of the fiber network simply by changing its peptide density.*

Self-assembly is one of the most active fields in chemistry and material science with more than 120000 references responding to this key word on Web of Science. When restricting the research to the two topics "surface-confined" and "self-assembly" only slightly more than 100 references remain and most of them address independently the two topics. This clearly demonstrates that the design of molecular systems that self-assemble spontaneously and exclusively at or near an interface represents a real scientific challenge. The most valuable approach developed so far to address this problem is to use non-self-assembling entities (molecules or macromolecules) that undergo a chemical change at the interface and thereby acquire a self-assembling propensity. Confining this chemical change at the interface can be achieved by using chemical reactions or physical processes catalyzed by molecular entities called morphogens (such as protons or metallic cations) that diffuse from the surface towards the solution, creating a concentration gradient, a strategy used by nature.[1] In synthetic approaches, the generation of these morphogens requires the continuous application of an external stimulus such as light[2] or electrochemistry[3] to maintain the self-assembly process.

In 2004, a new way to initiate gel formation in the bulk was introduced and called enzyme-assisted self-assembly (EA-SA).[4] The authors used alkaline phosphatase (ALP) to dephosphorylate a short Fmoc-protected peptide which becomes instantaneously an hydrogelator in the reaction medium due to the decrease of its water solubility. EA-SA was intensively developed by several groups who extended the concept to many more enzyme/peptide systems, getting success in fields such as inhibition of cancer cell lines,[5] intracellular imaging and intratumoral chemotherapy[6] or biocatalysis.[7] In 2009, the group of Ulijn grafted enzymes onto a substrate and observed the formation of localized peptide-based fibers originating from microscopic globules that were identified as enzyme clusters.[8]

Herein, we present the design of a new generation of surface localized EA-SA allowing the control of the hydrogel formation exclusively at and from a surface. The ability of the surface to initiate and to tune its own coating is based on the use of polyelectrolyte multilayer architectures that offer the possibility to design highly organized and enzymatically active nanometer size films.[9] Polyelectrolyte multilayers are organized structures obtained by the alternate deposition of polyanions and polycations onto a substrate.[10] They constitute an ideal tool to functionalize surfaces.[11] The general architecture we propose is represented in Figure 1 a. It is composed of three main film components: 1) a precursor multilayer deposited on the substrate, rendering the whole process substrate-independent; 2) an enzyme layer deposited onto the precursor layer and 3) a seed layer composed of polyelectrolytes modified by anchoring hydrogelator peptides. When precursor peptides, that is, peptides that do not interact with each other in solution, reach the multilayer, an enzymatic reaction occurs at the film/solution interface,[12] generating effective hydrogelator peptides at the film/solution interface. An increase of the concentration of hydrogelator peptides occurs near the film/solution interface and induces their spontaneous self-assembly initiated from, what can be called, a bioactive seed layer. Gel formation thus starts exclusively from the surface. Here, we demonstrate the validity of this approach and the control of the formation of

[*] C. Vigier-Carrière, Dr. T. Garnier, D. Wagner, Prof. P. Schaaf, Dr. F. Boulmedais, Dr. L. Jierry
Institut Charles Sadron, CNRS-UPR 22
23 rue du Loess, 67034 Strasbourg Cedex (France)
E-mail: schaaf@unistra.fr
fouzia.boulmedais@ics-cnrs.unistra.fr
Dr. P. Lavalle, Dr. M. Rabineau, Dr. J. Hemmerlé, Dr. B. Senger, Prof. P. Schaaf
INSERM Unité 1121 "Biomaterials and Bioengineering"
11 rue Humann, 67085 Strasbourg Cedex (France)

[**] C.V.-C. was supported by a fellowship from CNRS and Région Alsace. T.G. and D.W. acknowledge ANR (FORCELL, ANR-12-BSVE5-0021) for financial support. We gratefully acknowledge icFRC (Project Labex CSC-PSC-13), USIAS and IUF for financial support.

Supporting information for this article is available on the WWW under http://dx.doi.org/10.1002/anie.201504761.

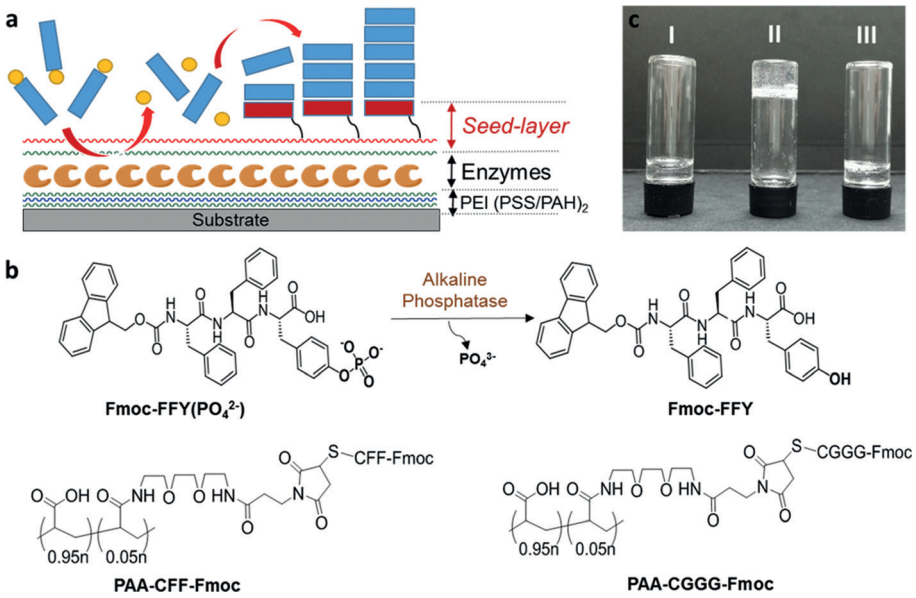

Figure 1. a) Representation of the surface-localized EA-SA concept. b) Chemical structures of all peptides and modified polyelectrolytes involved in this work (C = cysteine, F = phenylalanine, G = glycine, Y = tyrosine, Fmoc = fluorenylmethyloxycarbonyl). c) Gelation tests realized in vials with different solutions: I) 0.90 mM Fmoc-FFY(PO_4^{2-}) and ALP (1 U mL^{-1}); II) 0.60 mM Fmoc-FFY(PO_4^{2-}), PAA-CFF-Fmoc (0.30 mM of "CFF-Fmoc") and ALP (1 U mL^{-1}); III) 0.90 mM Fmoc-FFY(PO_4^{2-}), PAA and ALP (1 U mL^{-1}). The vials were turned upside down after 15 min.

a gel on the surface through the presence of the active seed layer.

Inspired by hydrogelator/enzyme systems introduced by Yang and Ulijn,[13] we designed an original peptide Fmoc-FFY(PO_4^{2-}) with a phosphorylated phenol group of the tyrosine at C-terminal position as model to validate our concept (Figure 1b). Alkaline phosphatase (ALP, 150 kDa) was used as catalytically active enzyme inducing the dephosphorylation of Fmoc-FFY(PO_4^{2-}) leading to the local production of the hydrogelator Fmoc-FFY.

The seed layer is composed of poly(acrylic acid) chains (PAA, 100 kDa) modified with the hydrogelator Fmoc-FFC through a short spacer (Figure 1b). The presence of the cysteine at C-terminal position allows clicking the peptide Fmoc-FFC through the thiol–ene reaction onto a maleimide-modified PAA. The grafting ratio of PAA-CFF-Fmoc is around 5% according to ^{1}H NMR spectroscopy. Syntheses and characterization of all compounds used in this work are reported in the Supporting Information (SI, Part 1). We first verified in solution 1) that gelation can be induced by dephosphorylation of Fmoc-FFY(PO_4^{2-}) in the presence of ALP, 2) that Fmoc-FFY, generated in situ, is an efficient hydrogelator, and 3) that PAA-CFF-Fmoc interacts with the peptide Fmoc-FFY, promoting gel formation. All the experiments were performed at 25 °C and at pH 9.5 using a borax buffer solution (SI, Part 2).

Next we wanted to validate the concept of seed layer acting as a "nucleating agent" and favoring the self-assembly of a gel on the surface. For this purpose we built a PEI-(PSS/PAH)$_2$-PAA-CFF-Fmoc film (PEI: poly(ethylene imine); PSS: poly(styrene sulfonate); PAH: poly(allylamine hydrochloride)) and brought it in contact with a solution containing Fmoc-FFY(PO_4^{2-}) at 0.90 mM and ALP at 0.33 mg mL^{-1} (or 1 U mL^{-1}). The process taking place at the interface was followed in situ by quartz crystal microbalance (QCM) by monitoring the evolution of the opposite of the fundamental resonance frequency shift $-\Delta f_1$ and the corresponding dissipation D_1. Whereas no gel is observed in solution under these conditions (Figure 1c), a strong increase of $-\Delta f_1$ is observed upon the injection of Fmoc-FFY(PO_4^{2-}) + ALP mixture up to a value of 1200 Hz after 8 min of build-up (Figure S1). In the same time, an important increase of the dissipation D_1 is measured, up to a high value of 900×10^{-6}. This indicates the formation of a thick viscoelastic gel on top of the multilayer. As a control experiment, the PAA-CFF-Fmoc seed layer was replaced by a modified PAA grafted with 5% of Fmoc-GGGC, a sequence recently described as an ideal non-gelating peptide (we also verified this result in solution; Figure S1).[14] When the Fmoc-FFY(PO_4^{2-}) + ALP mixture was brought in contact with a PAA-CGGG-Fmoc ended multilayer, only a small increase of the QCM signals was observed ($-\Delta f_1$ increases by 20 Hz and D_1 by 180×10^{-6}, Figure S1). When a PAA-CFF-Fmoc ended multilayer film was brought in contact with ALP in the absence of Fmoc-FFY(PO_4^{2-}), almost no variations of $-\Delta f_1$ and D_1 were observed by QCM (Figure S2). These results prove that the layer of PAA-CFF-Fmoc deposited on the multilayer serves indeed as an effective seed layer.

We then went one step further and tried to create a bioactive seed layer by incorporating the "reaction motor", that is, ALP, in the multilayer instead of having it in the solution. For this purpose, we built the multilayer architecture PEI-(PSS/PAH)$_2$-ALP-(PAH/PAA-CFF-Fmoc), represented in Figure 1a, and followed its build-up by QCM (Figure S3). The calculated thickness of this film is about 53 nm according to Sauerbrey's relation.[15] When this film was brought in contact with 0.90 mM of Fmoc-FFY(PO_4^{2-}) solution, an increase of $-\Delta f_1$ and D_1 occurred within 10 min after the injection of Fmoc-FFY(PO_4^{2-}) and reached respectively 1400 Hz and 1200×10^{-6} after 12 h (Figure 2a). This indicates the build-up of a gel at the interface. These values are even larger than those observed when ALP was in solution (Figure S1 in SI). When a Fmoc-FFY(PO_4^{2-}) solution (0.90 mM) was brought in contact with a film containing ALP and ending by PAA-CGGG-Fmoc, only a small increase of $-\Delta f_1$ (10 Hz) and of D_1 (135×10^{-6}) took place (Figure 2a). We verified, using *para*-nitrophenol phosphate as chromogenic enzyme substrate, that when PAA-CFF-Fmoc is replaced by PAA-CGGG-Fmoc the enzymatic activity of the film does not change (Figure S4). In order to get an idea

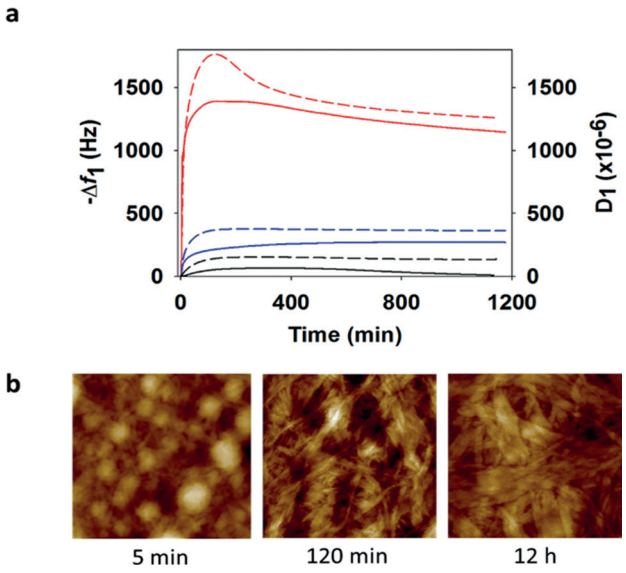

Figure 2. a) Comparison of the evolution of the $-\Delta f_1$ (full curve) and dissipation (dashed curve), measured by QCM-D, as a function of time when 0.90 mM Fmoc-FFY(PO_4^{2-}) solution is brought in contact with the multilayers PEI-(PSS/PAH)$_2$-ALP-(PAH/PAA-CFF-Fmoc) (red), PEI-(PSS/PAH)$_2$-ALP (blue), and (PEI-(PSS/PAH)$_2$-ALP-(PAH/PAA-CGGG-Fmoc) (black). b) Typical AFM images (1×1 μm^2), obtained in contact mode and dry state, of gel obtained after 5 min (*z*-scale = 76 nm), 120 min (*z*-scale = 40 nm), and 12 h (*z*-scale = 15 nm) of contact with Fmoc-FFY(PO_4^{2-}) solution.

about the synergy between the presence of the enzyme layer and the seed layer we performed also an experiment with the multilayer PEI-(PSS/PAH)$_2$-ALP ending with a bare enzyme layer. When bringing this film in contact with a Fmoc-FFY(PO_4^{2-}) solution at 1 mg mL^{-1} one observes an increase of $-\Delta f_1$ of 271 Hz. This shows that a "bare" enzyme layer allows getting a gel at the interface as first shown by Ulijn et al.[8] yet with a lesser efficacy. But the major drawback of the bare enzyme layer is the absence of possibility to tune and control the activity of this layer.

The gel build-up with a PAA-CFF-Fmoc seed layer was also followed by Fourier transform infrared spectroscopy in attenuated total reflection mode in deuterated water. After the injection of Fmoc-FFY(PO_4^{2-}), the intensities of the vibration bands at 1630 cm^{-1} and 1688 cm^{-1} increase and then level off after 60 min (Figure S5 in SI). The band at 1630 cm^{-1} corresponds to the carbonyl groups of the amide I involved in β-sheet assemblies[16,17] and the band at 1688 cm^{-1} can be assigned to carbamates present in the antiparallel β-sheets composed of Fmoc-FFY self-assembly.[18] A fluorescence spectroscopy study during the self-assembly of the gel shows the presence of Fmoc group excimer at 331 nm, in accordance with the β-sheet assembly characteristic of peptide-based hydrogel (Figure S6 in SI).[17] Using atomic force microscopy (AFM) in dry state, we imaged the obtained gel after 2, 5, 20, 120 min and 12 h of contact of Fmoc-FFY(PO_4^{2-}) solution with PEI-(PSS/PAH)$_2$-ALP-(PAH/PAA-CFF-Fmoc) film (Figure 2b and Figure S7). After 5 and 20 min, nanofibers appear over the whole coated substrate with entanglements and local bundles. After 120 min and 12 h, the nanofibrous structure appears as growing flat ribbons with a diameter of about 100 nm. Less than 5 min are necessary to the surface nucleation process to form fibers and the internal architecture of the gel changes over time despite the fact that the QCM signals level off after 20 min.

Confocal microscopy was used to determine the thickness of the gel after 12 h. PEI-(PSS/PAH)$_2$-ALP-(PAH/PAA-CFF-Fmoc) was spin-coated step-by-step on a glass substrate and then brought in contact for 12 h with a mixture of Fmoc-FFY(PO_4^{2-}) and fluorescein-labeled albumin (BSA^{FITC}). BSA^{FITC} was used for visualization purposes to be trapped in the gel during its growth. A gradient of fluorescence extending over several micrometers appears from the surface, suggesting a gradient of BSA^{FITC} and thus also of fiber density extending from the multilayer to the solution (Figure 3a).

Next, we looked at whether the concept of active seed layer allows to precisely control the film build-up by modifying the density of "Fmoc-FF" peptide moieties on the surface. This was done by adsorbing the seed layer from a solution containing a mixture of PAA-CFF-Fmoc and PAA-CGGG-Fmoc. Thus, the multilayer film PEI-(PSS/PAH)$_2$-ALP-(PAH/(PAA-CFF-Fmoc; PAA-CGGG-Fmoc)) was prepared with various mass ratios equal to $r = 0$, 0.25, 0.50, 0.60, 0.75 and 1.0 with r = [PAA-CFF-Fmoc]/([PAA-CGGG-Fmoc] + [PAA-CFF-Fmoc]). The value of $-\Delta f_1$ measured after 12 h for each ratio r is given in Figure 3b. By decreasing the proportion of PAA-CFF-Fmoc in the build-up solution of the seed layer, $-\Delta f_1$ corresponding to the gel build-up decreases correlatively. With r values below 1 after 12 h, the resulting gels show a less dense network of fibers, without formation of

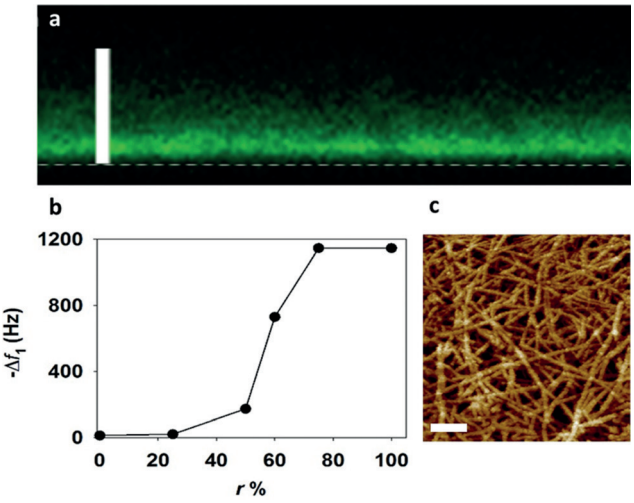

Figure 3. a) Confocal microscopy cross-section image of the gel self-assembled from Fmoc-FFY(PO_4^{2-}) on PAA-CFF-Fmoc seed layer ended film in the presence of BSA^{FITC}. The dashed line represents the substrate and the scale bar represents 5 μm. b) Evolution of $-\Delta f_1$ measured by QCM-D after 12 h of contact of PEI-(PSS/PAH)$_2$-ALP-(PAH/(PAA-CFF-Fmoc; PAA-CGGG-Fmoc)) with Fmoc-FFY(PO_4^{2-}) solution, as a function of the mass ratio r = [PAA-CFF-Fmoc]/([PAA-CGGG-Fmoc] + [PAA-CFF-Fmoc]) in the build-up solution. c) Typical AFM image (1×1 μm^2) obtained in contact mode and dry state after 12 h of self-assembly of gel from Fmoc-FFY(PO_4^{2-}) on multilayer ended with a ratio r = 75%. The *z* scale is 34 nm and the scale bar represents 0.15 μm.

large ribbons (Figure 3c). In addition, by decreasing the density of ALP in the multilayer, one observes correlatively a quasi linear decrease of the gel build-up kinetics when the film is brought in contact with the initiating Fmoc-FFY-(PO_4^{2-}) solution peptide (Part 3 in SI).

To sum up, we have introduced the concept of bioactive seed layer that triggers the build-up of a self-assembling peptide fiber network exclusively at the film/solution interface. Furthermore, by using confinement of enzymes through multilayer film design, the self-assembly process is maintained continuously and autonomously without any intervention of external stimuli. These two features render our concept fully original. In addition, the use of a bioactive seed layer allows controlling and tuning of both the network kinetics and the fiber morphologies. Currently, the research carried out in the field of self-assembly systems focuses on the development of increasingly complex architectures organized onto a surface, going closer to systems developed by nature. We believe that our bottom-up approach can significantly contribute to the design of sophisticated and smart nano-architecture systems.

Keywords: hydrogels · seed layers · self-assembly · thin layers

How to cite: *Angew. Chem. Int. Ed.* **2015**, *54*, 10198–10201
Angew. Chem. **2015**, *127*, 10336–10339

[1] G. Rydzek, L. Jierry, A. Parat, J. S. Thomann, J.-C. Voegel, B. Senger, J. Hemmerlé, A. Ponche, B. Frisch, P. Schaaf, F. Boulmedais, *Angew. Chem. Int. Ed.* **2011**, *50*, 4374–4377; *Angew. Chem.* **2011**, *123*, 4466–4469.

[2] C. Maity, W. E. Hendriksen, J. H. van Esch, R. Eelkema, *Angew. Chem. Int. Ed.* **2015**, *54*, 998–1001; *Angew. Chem.* **2015**, *127*, 1012–1015.

[3] a) X.-W. Shi, C.-Y. Tsao, X. Yang, Y. Liu, P. Dykstra, G. W. Rubloff, R. Ghodssi, W. E. Bentley, G. F. Payne, *Adv. Funct. Mater.* **2009**, *19*, 2074–2080; b) E. K. Johnson, D. J. Adams, P. J. Cameron, *J. Am. Chem. Soc.* **2010**, *132*, 5130–5136.

[4] Z. M. Yang, H. W. Gu, D. G. Fu, P. Gao, J. K. Lam, B. Xu, *Adv. Mater.* **2004**, *16*, 1440–1444.

[5] Y. Kuang, J. Shi, J. Li, D. Yuan, K. A. Alberti, Q. Xu, B. Xu, *Angew. Chem. Int. Ed.* **2014**, *53*, 8104–8107; *Angew. Chem.* **2014**, *126*, 8242–8245.

[6] J. Li, Y. Gao, Y. Kuang, J. Shi, X. Du, J. Zhou, H. Wang, Z. Yang, B. Xu, *J. Am. Chem. Soc.* **2013**, *135*, 9907–9914.

[7] Q. Wang, Z. Yang, Y. Gao, W. Ge, L. Wang, B. Xu, *Soft Matter* **2008**, *4*, 550–553.

[8] R. J. Williams, A. M. Smith, R. Collins, N. Hodson, A. K. Das, R. V. Ulijn, *Nat. Nanotechnol.* **2009**, *4*, 19–24.

[9] a) Z. Y. Tang, Y. Wang, P. Podsiadlo, N. A. Kotov, *Adv. Mater.* **2006**, *18*, 3203–3224; b) K. Ariga, T. Mori, J. P. Hill, *Chem. Sci.* **2011**, *2*, 195–203.

[10] a) G. Decher, *Science* **1997**, *277*, 1232–1237; b) J. Borges, J. F. Mano, *Chem. Rev.* **2014**, *114*, 8883–8942.

[11] K. Ariga, Y. Yamauchi, G. Rydzek, Q. M. Ji, Y. Yonamine, K. C. W. Wu, J. P. Hill, *Chem. Lett.* **2014**, *43*, 36–68.

[12] Y. Lvov, K. Ariga, I. Ichinose, T. Kunitake, *J. Am. Chem. Soc.* **1995**, *117*, 6117–6123.

[13] N. Javid, S. Roy, M. Zelzer, Z. Yang, J. Sefcik, R. V. Ulijn, *Biomacromolecules* **2013**, *14*, 4368–4376.

[14] P. W. J. M. Frederix, G. G. Scott, Y. M. Abul-Haija, D. Kalafatovic, C. G. Pappas, N. Javid, N. T. Hunt, R. V. Ulijn, T. Tuttle, *Nat. Chem.* **2015**, *7*, 30–37.

[15] G. Sauerbrey, *Z. Phys.* **1959**, *155*, 206–222.

[16] J. Kong, S. Yu, *Acta Biochim. Biophys. Sin.* **2007**, *39*, 549–559.

[17] A. M. Smith, R. J. Williams, C. Tang, P. Coppo, R. F. Collins, M. L. Turner, A. Saiani, R. V. Ulijn, *Adv. Mater.* **2008**, *20*, 37–41.

[18] a) S. Fleming, P. W. J. M. Frederix, I. Ramos Sasselli, N. T. Hunt, R. V. Ulijn, T. Tuttle, *Langmuir* **2013**, *29*, 9510–9515; b) N. Yamada, K. Ariga, M. Naito, K. Matsubara, E. Koyama, *J. Am. Chem. Soc.* **1998**, *120*, 12192–12199.

Received: May 26, 2015
Published online: July 14, 2015

